

The Luminescence Properties of Octahedral and Tetrahedral Molybdate Complexes

M. WIEGEL AND G. BLASSE

*Debye Research Institute, University of Utrecht, P.O. Box 80000,
3508 TA Utrecht, The Netherlands*

Received October 30, 1991; accepted March 13, 1992

The luminescence properties of MoO_4^{2-} and MoO_6^{0-} complexes are reported and discussed, using new data on La_2MoO_6 and ordered perovskites. In the molybdate complexes the probability of nonradiative return to the ground state decreases if the lowest absorption band is at higher energy and the Stokes shift decreases. In the perovskite $\text{Ba}_3\text{Y}_2\text{MoO}_9$, the Mo^{6+} and Y^{3+} ions show 1:2 ordering. A small amount of disorder is probably due to interchange of some of the Ba^{2+} and Y^{3+} ions. © 1992 Academic Press, Inc.

1. Introduction

In oxides the Mo^{6+} ion is usually four-coordinated. The most well-known and strongly luminescent molybdate is CaMoO_4 (1, 2). CaMoO_4 has the scheelite structure. The compound CaWO_4 is isostructural and isoelectronic. Its luminescence has a much higher quenching temperature than CaMoO_4 (1, 3). This has been ascribed to the fact that the excited states of tungstates are at higher energy than those of the molybdates. Actually the molybdate luminescence is close to the boundary between luminescent and non-luminescent compounds.

The compound La_2MoO_6 has a structure which consists of MoO_4 layers and La_2O_2 layers (3). The MoO_4 tetrahedra in the MoO_4 layers do not share oxygen atoms. La_2MoO_6 does not show luminescence at room temperature (RT) or at liquid nitrogen temperature (4). In the present work the luminescence of La_2MoO_6 is studied at liquid helium temperature (LHeT) in order to find an explanation for this behavior. There does not

exist an isostructural tungstate to make a comparison.

The number of studies on octahedral MoO_6^{0-} complexes is limited (5, 6). In order to elucidate the luminescence properties of the MoO_6^{0-} complex, the luminescence of MoO_6 groups in 1:1 ordered perovskites with general formula $A_2B\text{MoO}_6$ (7) is studied. In this structure the A^{2+} ions are in 12-coordination, whereas the B^{2+} and Mo^{6+} ions are in 6-coordination. The MoO_6 octahedra do not have oxygen ions in common because they are separated from each other by the B^{2+} ions. Such a crystal structure is an ideal model structure for the study of the octahedral molybdate complex. Van Oosterhout (8) has studied the octahedral tungstate complex in this lattice and found that it shows efficient luminescence with relatively small Stokes shift and pronounced concentration quenching at RT. Unfortunately the number of molybdates with ordered perovskite structure is restricted (7).

We also studied $\text{Ba}_3\text{Y}_2\text{MoO}_9$, which is a disordered perovskite according to (9). The

Eu^{3+} ion was used as a site probe to find the degree of disorder. The molybdate octahedra appear to be isolated from each other.

2. Experimental

2.1. Preparation

La_2MoO_6 was prepared by milling stoichiometric quantities of La_2O_3 (Highways International, 99.997%) and MoO_3 (Philips) followed by firing for 10 hr at 850°C in air. The product was milled again and fired for 4 hr at 1200°C . CaMoO_4 was synthesized as described in (1).

$\text{Ba}_2\text{CaMoO}_6$ was synthesized by firing an intimate mixture of BaCO_3 (Merck, p.a.), CaCO_3 (Merck, suprapur), and MoO_3 (molar ratio 2.03 : 1.015 : 1) at 850°C for 12 hr in air. This was followed by milling and firing for 2.5 hr at 1200°C . The preparation of $\text{Sr}_2\text{CaMoO}_6$ is similar. SrCO_3 (Merck, p.a.), CaCO_3 , and MoO_3 (molar ratio 2.05 : 1.025 : 1) were used as a starting mixture. In both preparations an excess of carbonates was used in order to avoid the formation of other phases like CaMoO_4 or BaMoO_4 .

$\text{Ba}_3\text{Y}_2\text{MoO}_9$ and $\text{Ba}_3\text{Y}_{1.99}\text{Eu}_{0.01}\text{MoO}_9$ were prepared as described in (9), using Y_2O_3 (Highways International, 99.999%) and Eu_2O_3 (Highways International, 99.99%).

All samples were checked by X-ray powder diffraction and found to be single phase.

2.2. Instrumentation

Optical measurements were performed on a Spex fluorolog spectrometer equipped with an Oxford helium cryostat and a Harwell temperature controller. The excitation spectra were corrected for the lamp intensity using a Rhodamin standard. The emission spectra were corrected for the photomultiplier sensitivity according to the curve given by the manufacturer.

For decay measurements a set-up consisting of a Molelectron DL-200 dye laser

pumped by a Molelectron UV-14 N_2 laser, in combination with a Spex 1704 X monochromator was used (11). With the aid of the dye PBBO (Exciton) $\text{Ba}_2\text{CaMoO}_6$ was excited at 400 nm.

3. Results

3.1. Luminescence of Molybdate Complexes

All compounds show broad, structureless emission bands in the red under UV excitation at 4.2 K. The emission and excitation bands do not overlap. The luminescence intensity is temperature dependent. At RT the present molybdates do not luminesce at all, in contrast to CaMoO_4 which does luminesce at RT. The results of the luminescence measurements are summarized in Table I.

As a representative example the emission and excitation spectra of the luminescence of $\text{Ba}_2\text{CaMoO}_6$ at 4.2 K are shown in Fig. 1. This molybdate has the most intense luminescence of the compounds under study. The emission is independent of the excitation wavelength. Due to the strong absorption of ultraviolet radiation, the excitation spectrum of molybdates cannot be used for interpretation.

Only for $\text{Ba}_2\text{CaMoO}_6$ the decay time has been measured. The other molybdates emit so weakly, that the decay time is determined by nonradiative processes. The decay time of the luminescence of $\text{Ba}_2\text{CaMoO}_6$ is rather long. At 4.2 K exponential curves were measured with a slope corresponding to a lifetime of 370 μsec . The temperature dependence of the decay time is given in Fig. 2.

3.2. $\text{Ba}_3\text{Y}_{1.99}\text{Eu}_{0.01}\text{MoO}_9$

The excitation spectrum of the Eu^{3+} emission ($\lambda_{\text{em}} = 614 \text{ nm}$) of $\text{Ba}_3\text{Y}_{1.99}\text{Eu}_{0.01}\text{MoO}_9$ consists of a strong broad band (350–450 nm) with a maximum at about 395 nm (molybdate absorption) and a number of less intense sharp lines (Eu^{3+} absorption).

TABLE I
LUMINESCENCE DATA OF MOLYBDATES AT 4.2 K

Compound	Luminescent center	Excitation max. (nm)	Emission max. (nm)	Stokes shift (10^3 cm^{-1})	$T_{1/2}^a$ (K)	Relative intensity ^b
La_2MoO_6	MoO_4	330	675	15.7	90	4
CaMoO_4	MoO_4	275	550	18.1	270 (1)	45
$\text{Ba}_2\text{CaMoO}_6$	MoO_6	400	600	8.3	60	10
$\text{Sr}_2\text{CaMoO}_6$	MoO_6	385	625	9.9	^c	3
$\text{Ba}_3\text{Y}_2\text{MoO}_9$	MoO_6	400	680	10.4	39	3

^a The temperature at which the luminescence intensity has decreased to 50% of the intensity at 4.2 K.

^b Relative to the luminescence intensity of $\text{Ba}_2\text{CaMoO}_6$ at 4.2 K.

^c Not measured.

In Fig. 3 the emission spectrum of the Eu^{3+} ion in $\text{Ba}_3\text{Y}_{1.99}\text{Eu}_{0.01}\text{MoO}_9$ ($\lambda_{\text{ext}} = 395 \text{ nm}$) is shown. The electronic ${}^5D_0 \rightarrow {}^7F_{0,1,2,3,4}$ transitions are observable. Although the emission lines are somewhat broad ($\approx 6 \text{ nm}$), the splitting of the lines is clear. At 4.2 K the molybdate emission is also observed. This emission consists of a broad band in the region 550–750 nm with a maximum at about 680 nm. At 200 K the molybdate emission is quenched, so that only the Eu^{3+} emission lines are observed.

4. Discussion

In molybdates the optical transitions are of the charge-transfer type (5). The spectra consist of broad emission and absorption bands. From the literature it is known that tetrahedrally coordinated Mo^{6+} (MoO_4^{2-}) has a larger relaxation than octahedrally coordinated Mo^{6+} (MoO_6^{6-}) ($\approx 17,000 \text{ cm}^{-1}$ vs $\approx 10,000 \text{ cm}^{-1}$) (5, 6). This is due to the fact that the Mo^{6+} ion is slightly too large for tetrahedral coordination and too small for octahedral coordination (5). This has also been observed for the tungstate luminescence. The Stokes shift data in Table I are in agreement with this.

The luminescence intensities given in Table I are measured for molybdate excitation, so that the absorption of the exciting radia-

tion is high and can be put equal for all samples. Therefore, these relative intensities are proportional to the quantum efficiencies (q). If we assume for the low temperature q of CaMoO_4 the same value as for CaWO_4 , viz. 80% (12), twice the values given in Table I are a reasonable estimate of q .

Furthermore Table I shows that the charge-transfer (CT) transitions on the molybdates are at a higher energy if the number of ligands decreases. This is a known feature of highly charged transition metal complexes with d^0 configuration (5), and a property of CT transitions in general.

4.1. The MoO_4^{2-} Complex in La_2MoO_6

At 4.2 K nonradiative decay dominates in the MoO_4 group of La_2MoO_6 . The quantum efficiency is low compared to that of the MoO_4 group in CaMoO_4 (1) (see also Table I). The lowest absorption band of La_2MoO_6 is at lower energy ($30,500 \text{ cm}^{-1}$) than that of CaMoO_4 ($34,500 \text{ cm}^{-1}$). The configurational coordinate diagram in Fig. 4 shows, that nonradiative decay depends on the vibrational wave function overlap (13) between the lowest vibrational level of the excited state e and a high vibrational level of the ground state g. The wave function of the lowest vibrational level is Gaussian, i.e., the most likely value of the configurational co-

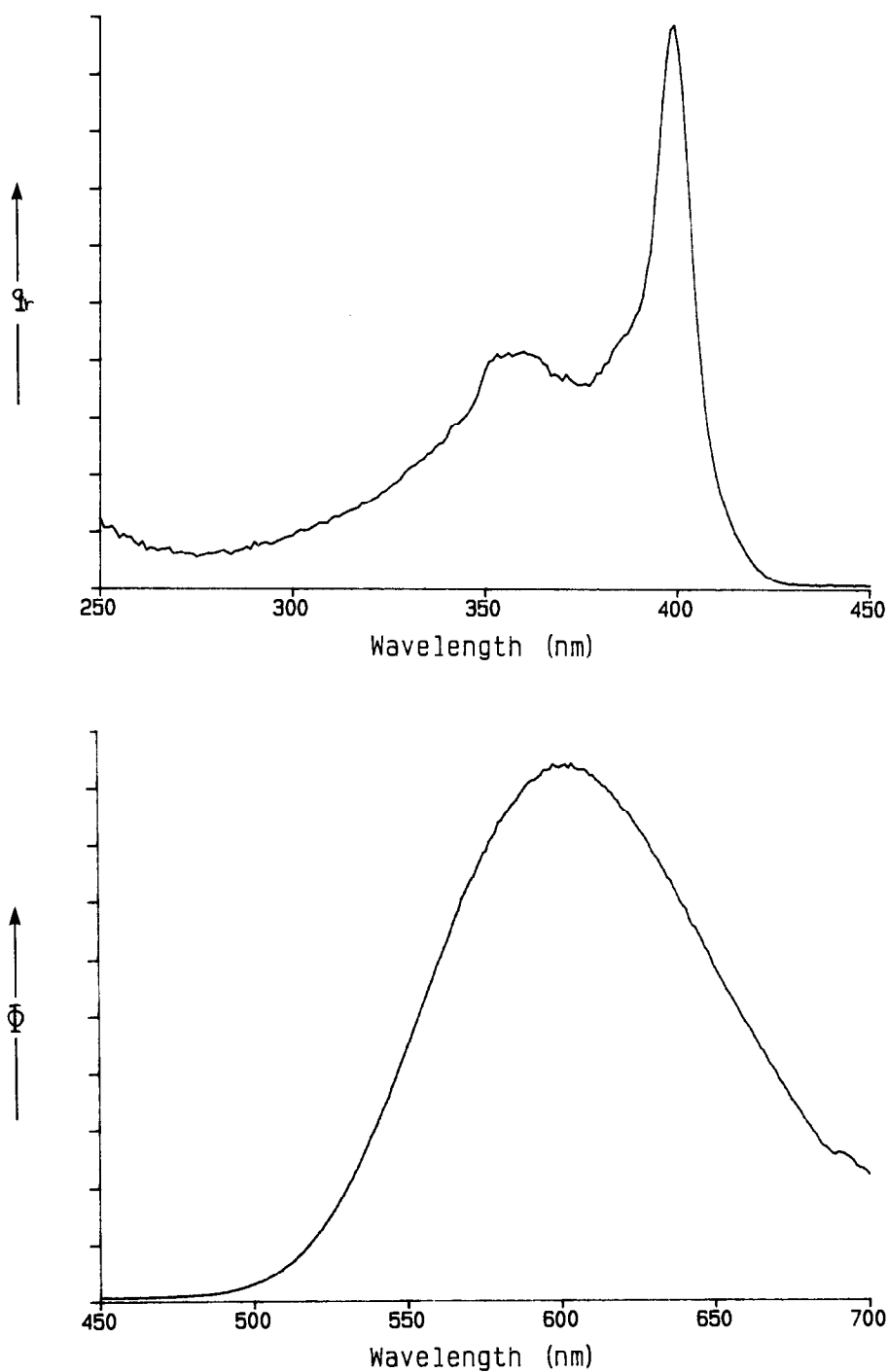


FIG. 1. The excitation and emission spectrum of the luminescence of $\text{Ba}_2\text{CaMoO}_6$ at 4.2 K. Φ gives the spectral radiant power per constant wavelength interval in arbitrary units. q_r is the quantum output in arbitrary units.

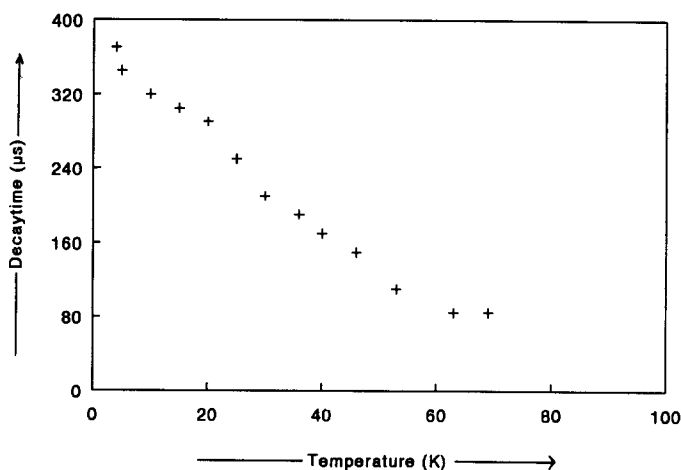


FIG. 2. The temperature dependence of the lifetime of the MoO_6^{2-} luminescence of $\text{Ba}_2\text{CaMoO}_6$, $\lambda_{\text{ext}} = 400 \text{ nm}$ and $\lambda_{\text{em}} = 606 \text{ nm}$.

ordinate Q is Q'_0 , whereas for the higher vibrational levels the most likely value of Q is at the edges of the parabola (13). Figure 4 shows that the vibrational wave function overlap will increase if parabola e shifts to the right (larger relaxation) or shifts downwards (lower absorption energy). This will lead to lower $T_{1/2}$ and lower luminescence efficiency. So the low luminescence efficiency and $T_{1/2}$ of La_2MoO_6 are ascribed to the low energy position of the optical absorption band. In the same way it has been explained why CaWO_4 has a higher luminescence efficiency and $T_{1/2}$ than CaMoO_4 (5).

A possible explanation for the low energy position of the CT state of La_2MoO_6 is the following. It is generally accepted that the CT transition in the MoO_4 group corresponds to a $t_1 \rightarrow 2e$ transition (1, 2). The molecular orbitals (MO's) with t_1 symmetry consist exclusively of π atomic orbitals (AO's) located on the oxygen ligands while the $2e$ MO's consists of d -type AO's ($d_{x^2-y^2}$, d_{z^2}) concentrated on the metal ion. In the scheelite structure of CaMoO_4 the Mo-O-Ca angle is about 130° , whereas the Mo-O-La angle in La_2MoO_6 is about 180°

(3, 4). This implies that in CaMoO_4 the π AO's on the oxygen ions are polarized by Ca^{2+} . In La_2MoO_6 this is not the case, because the π AO's do not point to the La^{3+} ion. As a consequence the lowest CT transition in La_2MoO_6 is indeed expected at a lower energy than in CaMoO_4 .

4.2. The MoO_6^{2-} Complex in Ordered Perovskites

The luminescence of the MoO_6 group in $\text{Ba}_2\text{CaMoO}_6$ is efficient compared with that of the MoO_4 group in La_2MoO_6 (see Table I), although the absorption band is at lower energy ($25,000 \text{ cm}^{-1}$ vs $30,500 \text{ cm}^{-1}$, respectively). The relaxation in octahedral complexes is smaller than in tetrahedral complexes (see Table I). Due to this the probability of nonradiative decay will decrease at low temperatures (see also the configurational coordinate diagram in Fig. 4). The emission and absorption bands do not overlap, so there cannot be effective energy migration at 4.2 K.

At higher temperatures energy migration can occur. For perovskite tungstates it has

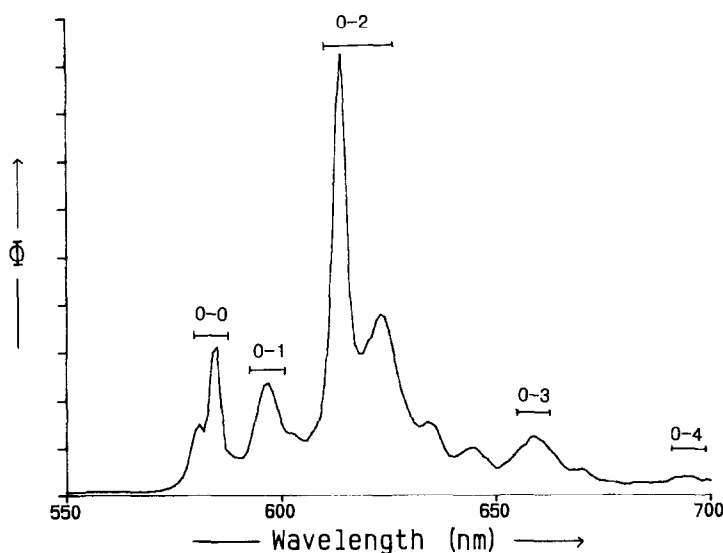


FIG. 3. Emission spectrum of $\text{Ba}_3\text{Y}_{1.99}\text{Eu}_{0.01}\text{MoO}_9$, recorded at 200 K, $\lambda_{\text{ext}} = 395$ nm. The notation 0-J indicates the ${}^5D_0 \rightarrow {}^7F_J$ transitions.

been shown that the quenching of the luminescence is due to energy migration (5).

Although the excited state of $\text{Sr}_2\text{CaMoO}_6$ is at higher energy, the luminescence efficiency is much lower compared with $\text{Ba}_2\text{CaMoO}_6$. This is ascribed to the larger Stokes shift. So the luminescence efficiency of the molybdates depends critically on the Stokes shift (14).

The luminescence of the MoO_6 group in $\text{Ba}_2\text{CaMoO}_6$ has a lifetime of 370 μsec . Because the quantum efficiency of the luminescence is considerably less than 100% (see Table I), the radiative decay time will be much longer than 370 μsec . This long decay time indicates that the transition must be forbidden. From the literature (5) it is known that the emitting level is a triplet state. Thus the transition can be ascribed to a spin-forbidden ${}^3T \rightarrow {}^1A$ transition.

With increasing temperature the luminescence intensity as well as the decay time (see Fig. 2) decrease. At higher temperatures the lifetime of the luminescence will be dominated by nonradiative processes.

4.3. $\text{Ba}_3\text{Y}_2\text{MoO}_9$

4.3.1. Disorder in $\text{Ba}_3\text{Y}_2\text{MoO}_9$. Since the halfwidth of the molybdate emission and excitation bands in $\text{Ba}_3\text{Y}_2\text{MoO}_9$ do not differ from those of the 1:1 ordered perovskite molybdates, it seems that there is only one type of MoO_6 octahedron present. The order in $\text{Ba}_3\text{Y}_2\text{MoO}_9$ was investigated in more detail by using Eu^{3+} as a probe.

In $\text{Ba}_3\text{Y}_{1.99}\text{Eu}_{0.01}\text{MoO}_9$ the Eu^{3+} ion occupies a lattice site without inversion symmetry, since the ${}^5D_0 \rightarrow {}^7F_2$ is strong (see Fig. 3). The Eu^{3+} emission lines are inhomogeneously broadened (≈ 6 nm), but the splitting of the lines is still observable. The emission spectrum in Fig. 3 shows that there are two types of Eu^{3+} centres in $\text{Ba}_3\text{Y}_{1.99}\text{Eu}_{0.01}\text{MoO}_9$, because the ${}^5D_0 \rightarrow {}^7F_0$ transition has two components. These transitions are relatively strong, due to a strong linear crystal field component. All these data are in agreement with a 1:2 ordered perovskite (10) with a slight disorder: the molybdate luminescence excludes molybdate-molybdate contacts (compare (15)); the 1:2 order

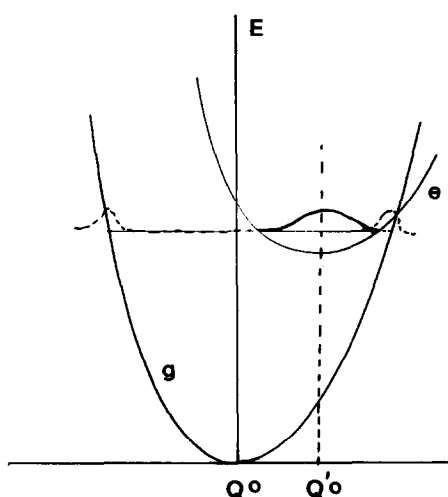


FIG. 4. Schematic configurational coordinate diagram illustrating a nonradiative transition; g indicates the ground state parabola and e the excited state parabola. The vibrational wavefunctions involved are indicated by a broken curve for g and a full curve for e.

has C_{3v} site symmetry for Y^{3+} (Eu^{3+}), which explains the strong 0-0 and 0-2 lines. The disorder and presence of two Eu^{3+} sites is then ascribed to an interchange of some Y^{3+} (Eu^{3+}) and Ba^{2+} ions.

4.3.2. MoO_6^{6-} complex in $Ba_3Y_2MoO_9$. The $T_{1/2}$ and the relative luminescence intensity of the MoO_6 group in $Ba_3Y_2MoO_9$ are low (see Table I) compared with Ba_2CaMoO_6 . As in the case of Sr_2CaMoO_6 this is ascribed to the large Stokes shift (see Section 4.1.).

5. Conclusion

Molybdate complexes have a higher luminescence intensity and $T_{1/2}$ if the lowest ab-

sorption band is at higher energy and the Stokes shift is smaller.

Acknowledgments

This work was supported by Philips Research Laboratories, Eindhoven. The authors thank Ms. E. M. Paardekoper, Mr. R. J. de Klein, and Mr. J. van Braak for performing part of the experiments.

References

1. J. A. GROENINK, C. HAKFOORT, AND G. BLASSE, *Phys. Status Solidi A* **54**, 477 (1979).
2. W. BARENDWAARD AND J. H. VAN DER WALLS, *Mol. Phys.* **59**, 337 (1986).
3. L. G. SILLÈN AND K. LUNDBORG, *Z. Anorg. Chem.* **252**, 2 (1943).
4. G. BLASSE AND A. BRIL, *J. Chem. Phys.* **45**, 2350 (1966).
5. G. BLASSE, *Struct. Bonding* **42**, 22 (1980).
6. G. BLASSE, G. J. DIRKSEN, AND H. SAUTEREAU, *Chem. Phys. Lett.* **78**, 234 (1981).
7. LANDOLT-BÖRNSTEIN, in "Kristallstruktur daten anorganischen Verbindungen" (W. Pies and A. Weiss, Ed.), Vol. 7f, Springer-Verlag, Berlin (1976).
8. A. B. VAN OOSTERHOUT, *Phys. Status Solidi A* **19**, 607 (1977).
9. J. W. TER VRUGT, W. L. WANMAKER, AND J. G. VERRIET, *J. Inorg. Nucl. Chem.* **34**, 762 (1972).
10. F. S. GALASSO, "Structure, Properties, and Preparation of Perovskite-Type Compounds," Pergamon Press, Oxford (1969).
11. J. P. M. VAN VLIET, G. BLASSE, AND L. H. BRIXNER, *J. Electrochem. Soc.* **135**, 1574 (1988).
12. G. BLASSE, *Eur. J. Solid State Inorg. Chem.* **28**, 719 (1991).
13. G. BLASSE, *Prog. Solid State Chem.* **18**, 79 (1988).
14. K. C. BLEIJENBERG AND G. BLASSE, *J. Solid State Chem.* **28**, 303 (1979).
15. J. G. H. BODE AND A. B. VAN OOSTERHOUT, *J. Lumin.* **10**, 237 (1975).